NEUROSCIENCE

Fibronectin in the olfactory mucus increases sensitivity of olfactory receptor response to odorants

Stella Chapman[1], Kenji Kondo[2], Sayoko Ihara[1], Chiori Ijichi[3], Kazushige Touhara[1]*, Koji Sato[1]*

Olfaction is a highly sensitive chemical detection system, but the origins of this sensitivity remain poorly understood. In terrestrial vertebrates, inhaled odorants diffuse through olfactory epithelial mucus (OEM) before activating olfactory receptors (ORs) on olfactory sensory neurons and initiating adenosine 3′,5′-monophosphate (cAMP)–mediated signaling. Impaired OEM secretion is associated with impaired olfactory sensitivity in humans and mice, but it remains unclear whether OEM directly improves sensitivity and whether specific active factors exist. Here, using a cAMP imaging–based heterologous OR expression assay, we demonstrate that fibronectin from human OEM increases the sensitivity of OR response to odorant. Fibronectin application partially restores electrical olfactory response of the mouse olfactory epithelium after OEM removal. In humans, OEM fibronectin levels are significantly decreased in patients with idiopathic olfactory disorder. These findings shed light on the role of OEM fibronectin in olfaction and may lead to sensitivity-enhancing additives for odorant sensors and treatments for hyposmia.

INTRODUCTION

Olfaction is a highly sensitive chemical sensing system that can detect many thousands of different volatile chemicals at parts-per-trillion level. This process begins when odorants in the nasal airway dissolve into the olfactory epithelial mucus (OEM), an aqueous layer that covers the olfactory epithelium. Odorants then bind cognate olfactory receptors (ORs), which, in vertebrates, are G protein–coupled receptors (*1*) expressed on the cilia of olfactory sensory neurons (OSNs). Binding of odorant to cognate OR initiates signaling via $G_{\alpha olf}$, resulting in a rise in intracellular adenosine 3′,5′-monophosphate (cAMP) and the generation of action potentials. While the intracellular olfactory signaling components have been successfully reconstituted in heterologous cell systems, allowing for detailed molecular characterization of ORs, this reconstruction has proven insufficient to replicate in vivo olfactory selectivity and sensitivity (*2*–*4*).

In vivo, ORs are surrounded by OEM, which contains hundreds of biomolecules (*5*–*9*). OEM plays multiple roles, including shielding the olfactory epithelium from pathogens and desiccation and modulating olfactory selectivity via odorant-metabolizing enzyme activity (*3*). OEM has also long been suspected to play a role in olfactory sensitivity, since, when OEM secretion is impaired, both human patients (*10*–*12*) and mice (*13*) show decreased olfactory sensitivity compared to healthy individuals. While these results suggest that sensitivity-enhancing factors exist in OEM, neither direct evidence of improvement in olfactory sensitivity by OEM nor identification of an active factor has yet been reported.

The vertebrate odorant binding proteins (OBPs), a group of lipocalins expressed in the OEM, are often raised as candidate sensitivity-enhancing factors because they bind some odorants in vitro (*14*, *15*). Rodent studies have demonstrated a role for OBPs in the vomeronasal system (*15*), an auxiliary chemosensory system present in a subset of nonhuman animals. In the main olfactory system, roles for OBPs in transporting odorants to the receptor and thereby increasing sensitivity, as well as in other processes such as odorant scavenging and disposal, have been proposed (*14*, *15*). However, the few reported tests of the effect of vertebrate OBPs on odorant response show conflicting results (*16*, *17*). Hence, the function of OBPs in the main olfactory system remains unclear.

With the aim of understanding the relationship between OEM and sensitivity, we asked whether OEM can directly improve the sensitivity of ORs to odorants and, if so, which factors are involved. To screen OEM for sensitivity-enhancing factors, we developed a cAMP imaging technique that allows spatiotemporal analysis of cAMP response dynamics evoked by ORs in heterologous cells. Using this technique, we found that fibronectin (FN) secreted into the human OEM is an olfactory response–enhancing factor with activity on odorants from multiple chemical classes. Our results, obtained both from our heterologous cell assay and from electrical recording from the olfactory epithelium, demonstrate that specific factors within OEM are involved in increasing olfactory sensitivity and pave the way for treatment of hyposmia and improvement of the sensitivity of biohybrid odorant sensors.

RESULTS

OR-expressing human embryonic kidney–293T/cAMPr cells allow visualization of odorant-induced cAMP response dynamics

The first downstream signal of the olfactory response is a rise in intracellular cAMP, but kinetic analysis of odor-evoked cAMP responses with high spatiotemporal resolution has not yet been reported. Thus, to visualize the spatiotemporal dynamics of OR-induced changes in intracellular cAMP concentration, we established the human embryonic kidney (HEK) 293T/cAMPr cell line, which stably expresses a cpGFP-based single-wavelength cAMP sensor, cAMPr (*18*). We confirmed the expression of cAMPr in HEK293T/cAMPr cells by cAMPr fluorescence (fig. S1A).

We next tested whether HEK293T/cAMPr cells expressing ORs displayed the typical characteristics of the OR/odorant-induced cAMP response. To this end, we first tested whether HEK293T/

[1]Laboratory of Biological Chemistry, Department of Applied Biological Chemistry, The University of Tokyo, Tokyo 113-8657, Japan. [2]Department of Otorhinolaryngology-Head and Neck Surgery, Graduate School of Medicine and Faculty of Medicine, The University of Tokyo, Tokyo 113-8655, Japan. [3]Food Products Division, Technology & Solution Development Center, Institute of Food Science and Technologies, Ajinomoto Co. Inc., Kawasaki 210-8681, Japan.
*Corresponding author. Email: ktouhara@g.ecc.u-tokyo.ac.jp (K.T.); satok@g.ecc.u-tokyo.ac.jp (K.S.)

cAMPr cells expressing a eugenol-responsive mouse OR, Olfr73 (mOR-EG), showed an increase in cAMPr fluorescence upon stimulation with eugenol. We confirmed that 1-min eugenol stimulation induced an increase in cAMPr fluorescence (fig. S1B). Under physiological conditions, OSNs can respond to short pulse stimulation of odorants. Thus, we next confirmed that 0.1-s odorant stimulation triggers a sustained cAMP increase (fig. S1C) and that longer odor exposure triggers larger cAMP responses, again using Olfr73-expressing HEK293T/cAMPr cells (Fig. 1A and fig. S1C).

We further confirmed that the amplitude of cAMP response of Olfr73 increased in a dose-dependent manner. We found a median effective concentration (EC_{50}) of 154 μM and a Hill coefficient of 0.677 (Fig. 1, B and C), which are similar to previously reported cAMP measurements of the Olfr73 response to eugenol (*19*). We further examined the cAMP response dynamics of human ORs (Fig. 1, D and E). As with Olfr73-expressing HEK293T/cAMPr cells, OR2W1-expressing HEK293T/cAMPr cells and OR5AN1-expressing HEK293T/cAMPr cells showed cAMP responses upon stimulation with their cognate odorant [pentyl acetate (PA) or musk ketone, respectively], with response amplitude increasing in a dose-dependent manner. The establishment of the HEK293T/cAMPr cells allowed us to analyze cAMP response dynamics to odorant stimulation in real time and with high temporal resolution for a broad selection of ORs.

Human OEM sample enhances OR-evoked cAMP responses to odorant

To examine whether OEM can modulate OR response, we used HEK293T/cAMPr cells to test the effect of human OEM sample application on the response of human ORs to their cognate odorants (Fig. 2). Using a PA-responsive OR, OR2W1, we measured the response to PA stimulation before and after application of OEM sample (Fig. 2, A and B). We found that the amplitude of the response to PA immediately after OEM sample application was 1.4× greater than the response before OEM application and that subsequent responses returned to baseline levels. This response enhancement suggested that OEM contains factors that affect OR response to odorants.

The presence of bulk protein may affect odorant bioavailability and thus affect the odorant response. OEM samples obtained by our method contain ~500 μg/ml of total protein (*9*). To determine whether response enhancement was caused by the increase in bulk protein, we next tested the effect of bovine serum albumin (BSA) at a concentration matched to OEM total protein. We found that application of BSA did not significantly change the amplitude of the OR2W1 response to PA (Fig. 2, C and D). We further tested the dependency of OEM-mediated response enhancement on the dilution level of OEM sample and found that with increasing dilution of OEM sample, the response-enhancement effect decreased (Fig. 2E and fig. S2). These results indicated that specific factor(s) in the OEM sample were responsible for response enhancement.

Human ORs are encoded by a ~400-member multigene family and recognize chemically diverse odorant molecules. To determine whether OEM-mediated response enhancement was specific to the OR2W1/PA OR-odorant pair, we next tested OEM with two other human OR-odorant pairs: OR5K1/2,3-dimethyl pyrazine and OR5AN1/musk ketone. The odorants used come from different chemical classes: PA is an ester, 2,3-dimethyl pyrazine is a pyrazine, and musk ketone

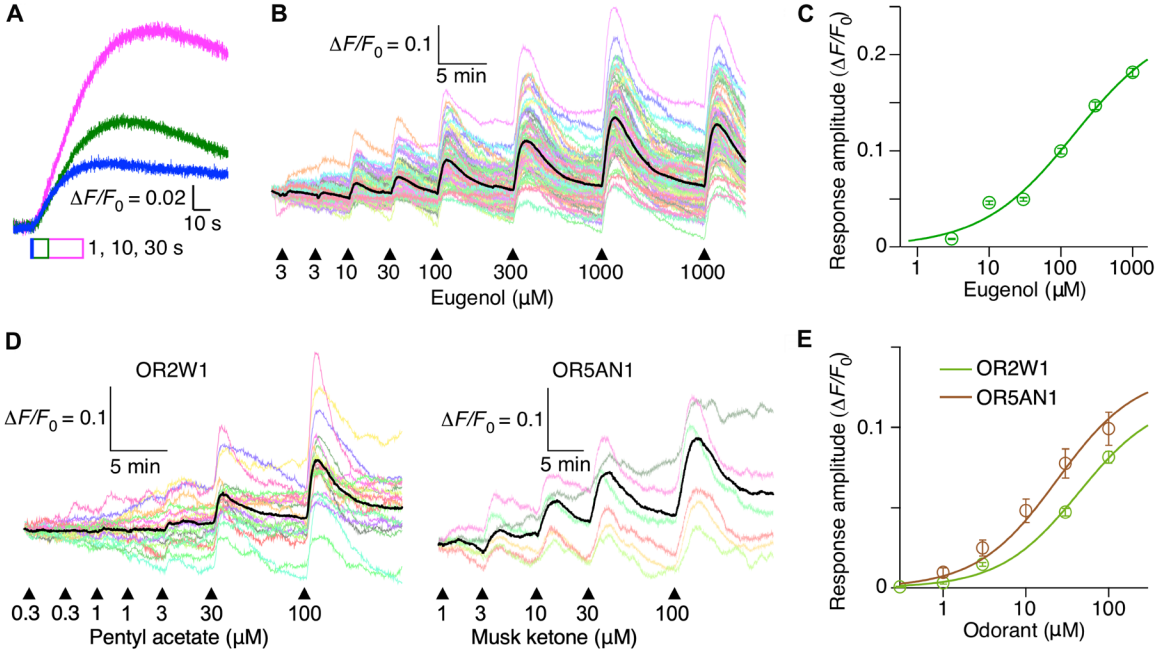

Fig. 1. Odorant-induced cAMP responses of mammalian ORs in HEK293T cells stably expressing cAMPr. (**A**) Representative traces of $\Delta F/F_0$ of cAMPr in an Olfr73-transfected cell stimulated with 300 μM eugenol. Duration of odorant stimulation is indicated by bars. (**B**) Examples of concentration dependence of cAMP responses to eugenol in Olfr73-expressing HEK293T/cAMPr cells ($n = 76$). Black trace indicates the average waveform of colored traces, which indicate the responses of individual cells. Arrowheads indicate the timing of 10-s stimulation of eugenol at indicated concentrations. (**C**) Concentration-response curve of Olfr73 to eugenol. Data are obtained from three independent experiments ($n = 189$ cells). Circles indicate averages. Error bars indicate ±SEM. (**D**) Examples of concentration dependence of cAMP responses to odorants in human OR (OR2W1, $n = 21$; OR5AN1, $n = 8$) expressing HEK293T/cAMPr cells. (**E**) Concentration-response curves of OR2W1 to PA (green) and OR5AN1 to musk ketone (brown). Data are obtained from three independent experiments per OR (OR2W1, $n = 68$ cells; OR5AN1, $n = 21$ cells). Circles indicate averages. Error bars indicate ±SEM. For OR2W1, the EC_{50} was 44.0 μM, and the Hill coefficient was 0.91. For OR5AN1, the EC_{50} was 23.8 μM, and the Hill coefficient was 0.90.

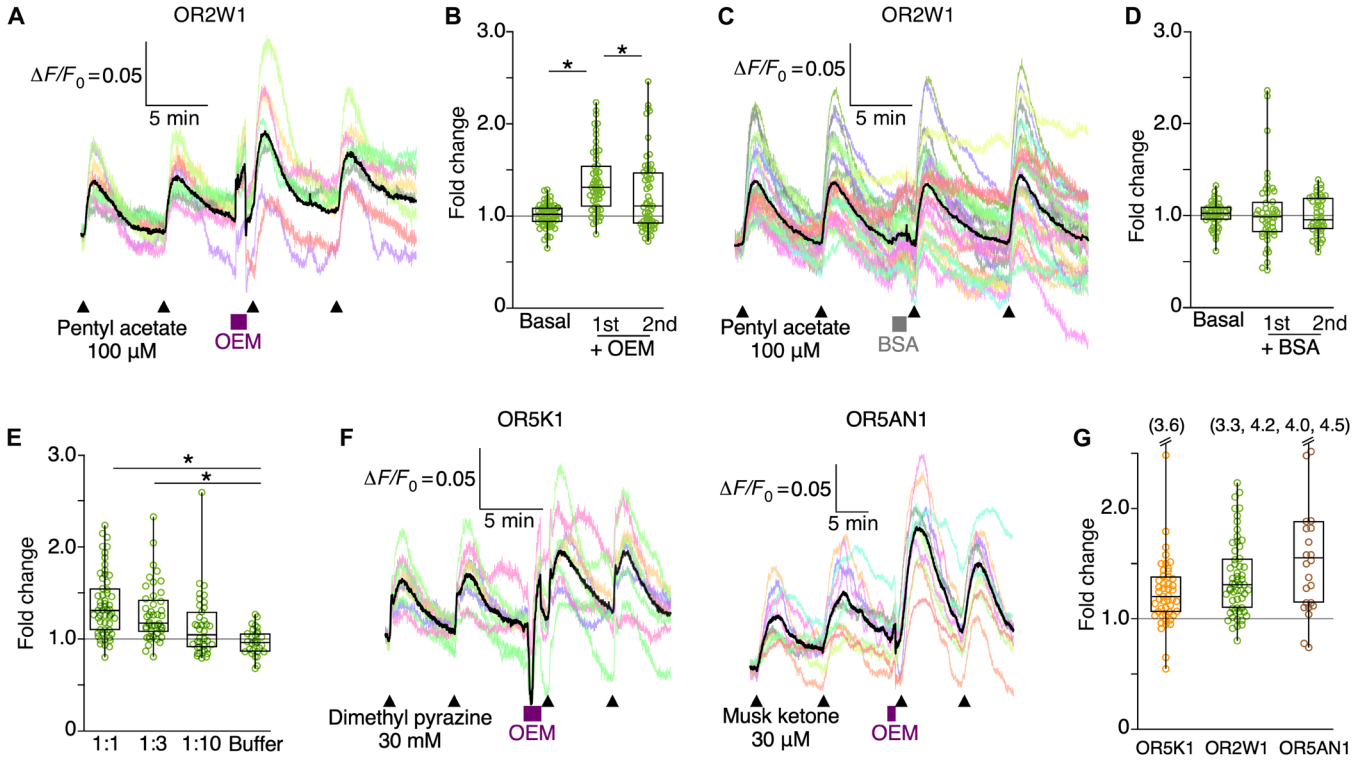

Fig. 2. Enhancement of odorant response by human OEM sample. (**A**) Representative cAMP responses to 100 μM PA in OR2W1-expressing HEK293T/cAMPr cells ($n = 8$) before and after 1-min application of human OEM sample. (**B**) Fold change of amplitude of PA–evoked response before and after OEM sample application. Data were obtained from seven independent experiments ($n = 57$ cells). Circles indicate values for individual cells. Basal ratio indicates ratio of pre-OEM response amplitudes, first ratio indicates ratio of first post-OEM response to last pre-OEM response, and second ratio indicates ratio of second post-OEM response to last pre-OEM response. (**C**) Representative cAMP responses to 100 μM PA in OR2W1-expressing HEK293T/cAMPr cells ($n = 29$) before and after application of BSA at 500 μg/ml to match the total protein concentration in the OEM sample. (**D**) Fold change of amplitude of PA-evoked response before and after BSA for 45 cells recorded across three independent experiments. (**E**) Dose-effect relationship between OEM sample dilution level and fold change of OR2W1 response to 100 μM PA upon sample addition. "Undiluted" data are ratio 1 of (B). Dilution data of 1:3 are from 36 cells recorded across three independent experiments. Dilution data of 1:10 are from 38 cells recorded across four independent experiments. Buffer-only data are from 29 cells recorded across three independent experiments. (**F**) Representative cAMP responses to indicated odorant in HEK293T/cAMPr cells expressing human ORs (OR5K1, $n = 10$; OR5AN1, $n = 11$) before and after application of human OEM sample. (**G**) Comparison of fold change of odor-evoked response amplitude upon addition of OEM sample (first ratio) for three human ORs and their cognate odorants. OR5K1 data are from 50 cells recorded across four independent experiments. OR5AN1 data are from 25 cells recorded across three independent experiments. In all panels, $^*P < 0.05$, post hoc Tukey test with one-way analysis of variance (ANOVA).

is an aromatic; the three ORs are from different phylogenetic groups (*20*). We found that, as with OR2W1/PA, application of OEM sample increased odorant response for both OR-odorant pairs (Fig. 2, F and G). Response enhancement across three chemically different pairs suggested that the effect might be general across many ORs and odorants.

FN is an odorant response–enhancing factor in human OEM

Having found that OEM can enhance OR response to odorants, we next set out to identify the active factor. First, to determine the molecular weight range of the factor, we performed ultrafiltration. We found that the >100-kDa fraction had activity and the <100-kDa fraction did not (Fig. 3, A to C). Although the OEM also contains small molecules, lipids, and glycans, this high molecular weight suggested a protein. Using proteomics data from human OEM and respiratory mucus samples (*9*), we examined the abundance of proteins >100 kDa (Fig. 3D, red circles). We found that among these proteins, FN was the most abundant in the OEM. Furthermore, FN was scarce in the respiratory mucus, suggesting an OEM-specific function. We thus hypothesized that FN might be the active factor in OEM.

To test this hypothesis, we next partially purified FN from the OEM sample by affinity purification on gelatin-Sepharose (Fig. 3E). We found that the affinity-purified FN enhanced odorant response (eluate; Fig. 3, F and H), while the flow through from purification, which contained almost no FN, did not (Fig. 3, G and H). These results indicate that FN in OEM has olfactory response–enhancing activity.

We further determined the concentration of FN in human OEM. We obtained OEM samples from 39 normosmic volunteers [Table 1, Normosmic (all)] and found that FN comprised ~1% of the total protein in the sample: 0.024 μg/2.5 μg of total protein, with no significant differences between female and male individuals (Fig. 3I). Since the total protein in these OEM samples is, on average, 430 μg/ml, a value that we estimate to be 20× diluted from OEM in the nose (*9*), we estimate the FN concentration in the OEM in vivo to be on the order of 20 to 100 μg/ml.

Next, we tested whether FN in and below this concentration range showed odorant response enhancement in our heterologous OR

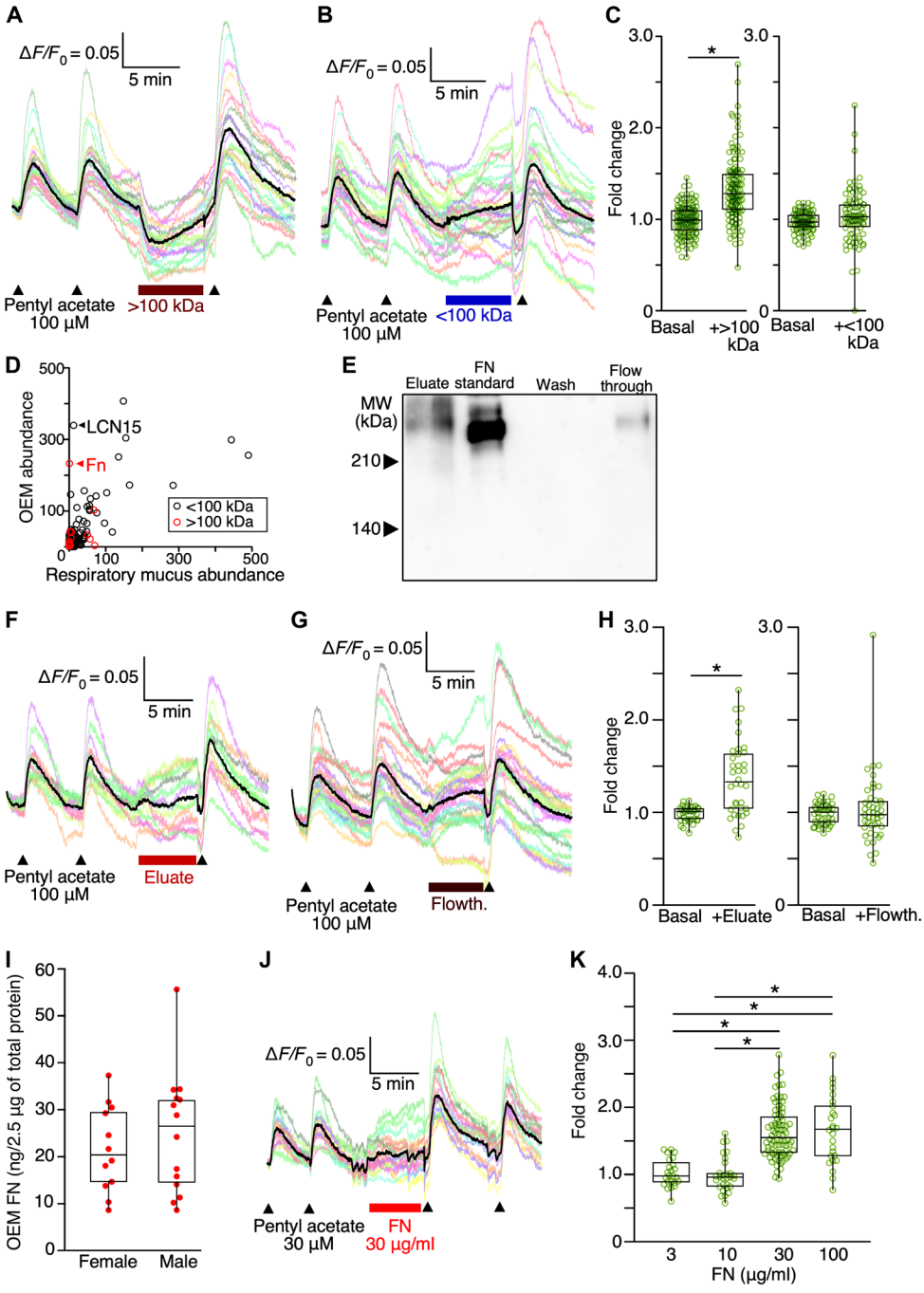

Fig. 3. Enhancement of odorant responses by FN in human olfactory mucus. (**A**) Representative cAMP responses to PA in OR2W1-expressing HEK293T/cAMPr cells ($n = 23$) before and after application of >100-kDa fraction of OEM sample. (**B**) Representative cAMP responses to PA in OR2W1-expressing HEK293T/cAMPr cells ($n = 28$) before and after application of <100-kDa OEM fraction. (**C**) Fold change of PA response amplitude before and after application of indicated sample. Circles indicate values for individual cells. Basal ratio indicates ratio of presample responses. Five independent experiments ($n = 133$ cells) for >100kDa; three independent experiments ($n = 90$ cells) for <100 kDa. *$P < 0.05$ (unpaired *t*-test). (**D**) Abundance in human OEM versus respiratory mucus for 359 proteins. Proteins >100 kDa are shown as red circles, and proteins <100 kDa are shown as black circles. (**E**) Anti-FN Western blot of eluate and flow through. Standard is commercial FN. MW, molecular weight. (**F**) Representative cAMP responses to PA in OR2W1-expressing HEK293T/cAMPr cells ($n = 13$) before and after application of gelatin affinity-purified FN (eluate). (**G**) Representative cAMP responses to PA in OR2W1-expressing HEK293T/cAMPr cells ($n = 25$) before and after application gelatin affinity column flow through (flowth.). (**H**) Fold change of PA response amplitude before and after application of indicated sample; three independent experiments per sample (eluate, $n = 36$ cells; flow through, $n = 44$ cells). *$P < 0.05$ (unpaired *t*-test). (**I**) OEM FN levels in normosmic volunteers (19 female and 20 male), normalized to total protein in sample. $P = 0.55$ (unpaired *t*-test). (**J**) Representative cAMP responses to 30 μM PA in OR2W1-expressing HEK293T/cAMPr cells ($n = 20$) before and after application of FN (30 μg/ml). (**K**) Dose-effect relationship between concentration of applied FN and fold change of OR2W1 response upon sample addition. Three independent experiments per concentration (100 μg/ml, $n = 26$ cells; 30 μg/ml, $n = 81$ cells, 10 μg/ml, $n = 29$ cells; 3 μg/ml, $n = 24$ cells). *$P < 0.05$, post hoc Tukey test with one-way ANOVA.

Table 1. Demographic and olfactory characteristics of human individuals who provided olfactory mucus samples.

	Idiopathic olfactory disorder (IOD) group	Normosmic group (age-matched controls)	Normosmic (all)
Age range (years)	47–83	46–84	26–84
Mean age ± SD (years)	70 ± 12	70 ± 12	52 ± 21
Sex (*n*, female/male)	9/7	8/8	19/20
Smoker (*n*, current/former/nonsmoker)	0/5/11	1/5/10	1/5/33
T&T threshold	5.1 ± 0.9	≤2.0	≤2.0
OEM FN concentration, means ± SD (ng/2.5 μg of protein)	14.3 ± 7.7	23.3 ± 12	23.0 ± 13

assay (Fig. 3, J and K, and fig. S3). We found that significant odorant response enhancement could be seen from FN (30 μg/ml), indicating that FN at the concentrations found in the OEM in vivo shows activity. Since we did not see a significant difference between the fold enhancement at 30 μg/ml and that at 100 μg/ml under our experimental conditions (Fig. 3K), we used 30 μg/ml for subsequent experiments.

FN has an odorant-dependent effect on OR response sensitivity

FN is known to interact with many proteins, including integrins on the cell membrane, as well as with small molecules (*21*). Thus, both ORs and odorants are potential molecular interaction partners. To examine which might be the interaction partner of FN, we next compared the effect of FN on odorant response across a broader set of odorant-human OR pairs: 10 odorants and 8 ORs (Fig. 4).

To compare the effect on odorant response across pairs, we took the dose-response curve before and after FN application (Fig. 4A). We found that for 10 of 11 pairs, FN decreased EC_{50} (Fig. 4A and Table 2); for one pair, OR8D1/sotolon, we did not detect a change. We also found that at low odorant concentrations, FN increased the percentage of OR-expressing cells with a detectable odorant response (Fig. 4B and table S1), even for the pair for which we did not detect a change in EC_{50}, OR8D1/sotolon.

We noticed that the degree of EC_{50} decrease varied across OR-odorant pairs (Fig. 4A and Table 2). To test whether FN acts on the OR or on the odorant, we compared the EC_{50} decrease for two different odorants recognized by the same OR. We performed this comparison for three ORs—OR8D1, OR2W1, and OR5AN1—and found that even for the same receptor, the EC_{50} decrease varied depending on the odorant (Fig. 4A, shaded boxes). Markedly, for OR8D1, EC_{50} decrease was detected for one cognate odorant, cyclotene, and not for the other, sotolon. These odorant-dependent differences in EC_{50} decrease suggest that FN acts on the odorant, not the OR.

Next, we tested whether the effect on EC_{50} for a given odorant was dependent on the identity of the OR. Using the odorant γ-undecalactone, we compared the effect of FN on odorant response for two ORs from distinct phylogenetic subfamilies, OR1D2 and OR2J2. Both ORs showed a similar 2.5-fold EC_{50} decrease upon addition of FN (Fig. 4A, outlined box). This OR-independent effect on EC_{50} for a given odorant is consistent with an OR-independent mechanism of action for FN.

To examine which odorant characteristics were important for interaction with FN, we examined the correlation between odorant physicochemical properties and FN-mediated EC_{50} fold decrease. Classically, hydrophobicity and vapor pressure have been considered critical properties for odorant recognition (*22*). We found that odorant hydrophobicity, as measured by log $P_{octanol/water}$ ($P_{o/w}$), showed a significant strong positive correlation with EC_{50} fold decrease (Fig. 4C). The only odorant for which an EC_{50} shift was not detected, sotolon, has the lowest log $P_{o/w}$ of those tested. Odorant boiling point also showed a positive correlation with EC_{50} fold decrease (fig. S4A). However, neither vapor pressure nor odorant molecular weight showed a significant correlation with EC_{50} fold decrease (fig. S4, B and C). In summary, FN has an odorant-dependent effect on olfactory sensitivity, with stronger effects on more hydrophobic odorants.

FN affects response to odorants by increasing amount of odorant proximal to cells

If FN interacts with odorants and not ORs, then the FN-induced increase in sensitivity of OR-expressing HEK293T/cAMP cells to odorants can occur in three possible ways: (i) an increase in odorant concentration proximal to ORs, (ii) slower diffusion of odorants proximal to ORs, or (iii) both of the above. To determine which of these occurred with FN, we monitored odorant concentration around cells using the autofluorescent odorant, methyl anthranilate (MA). MA fluorescence excitation and emission are distinct from those of cpGFP (*23*), allowing simultaneous imaging of odorant fluorescence and response of its cognate receptor, OR5P3 (fig. S5). In addition, this odorant-receptor pair is well suited for studying the FN effect, since FN evokes a threefold EC_{50} decrease (Fig. 4A).

Using an odorant concentration within the range for which we could observe both readily detectable odorant fluorescence and FN-mediated response enhancement, we tested the effect of FN on the odorant fluorescence and response to odorant, measuring both the response of individual cells and the local odorant fluorescence around each cell (Fig. 5, A and B). We found that, concomitant with the 1.5× fold increase in odorant response (Fig. 5C), odorant fluorescence around cells also increased by 1.4× on average (Fig. 5D). This increase in local odorant fluorescence suggests that FN increases the amount of odorant and/or decreases diffusion of odorants around cells.

Next, we examined whether FN affected odorant removal from the surface of cells, which correlates with the rate of odorant diffusion proximal to ORs. If FN decreases odorant diffusion rate, then odorant fluorescence around the cells should persist longer for the post-FN odorant application than for the pre-FN odorant application. To quantify the duration for which odorants persist around cells, we fit the decay phase of the odorant fluorescence waveform for the pre-FN stimulation and for the post-FN stimulation (Fig. 5E)

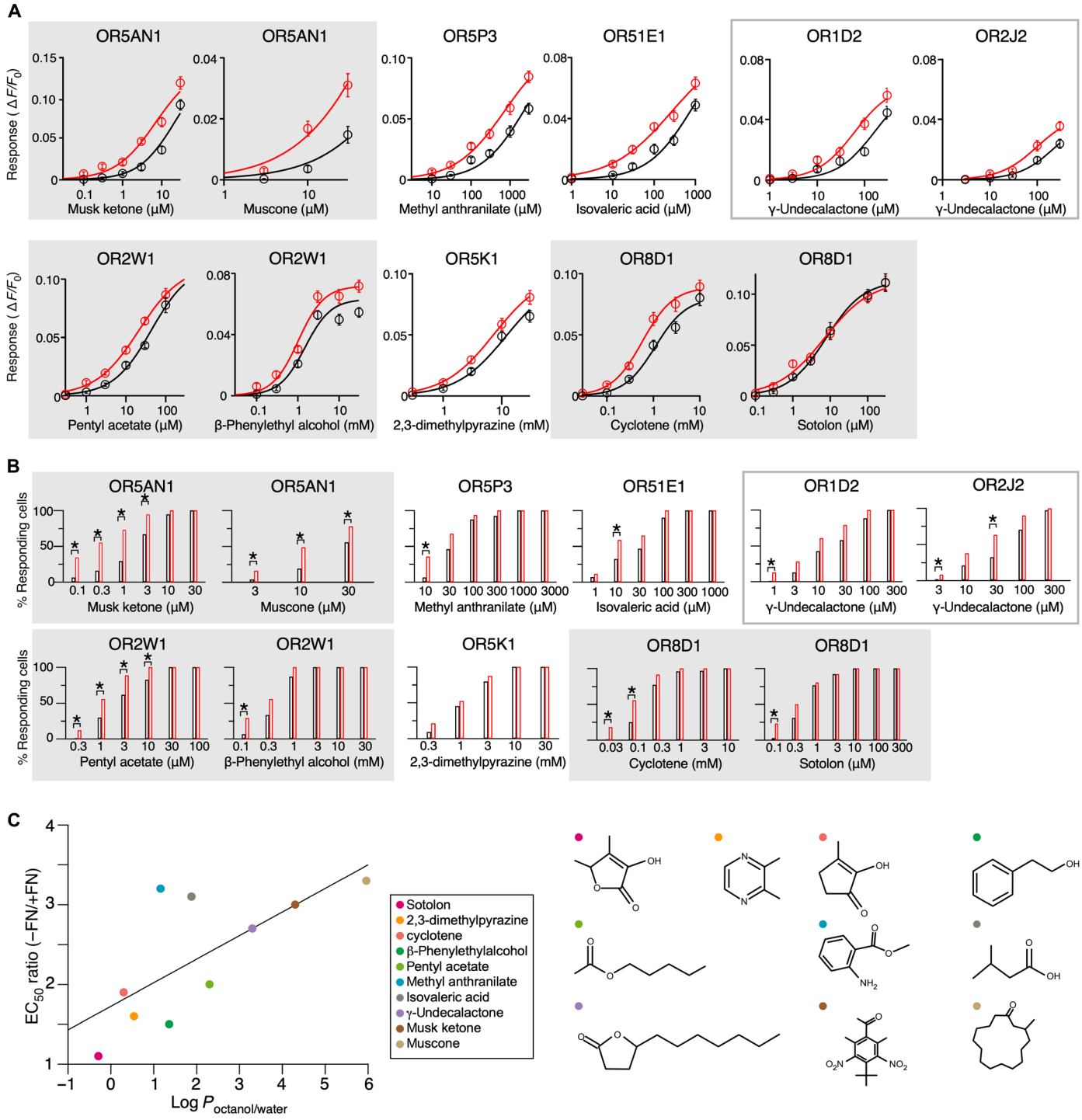

Fig. 4. FN-mediated sensitivity enhancement for 10 odorant-OR pairs. (**A**) Concentration dependence curves of responses of human OR-expressing HEK293T/cAMPr cells to the indicated cognate odorants before (black circles) and immediately after (red circles) FN addition. Circles represent the average of at least 20 cells measured across three to five independent experiments. Error bars represent ±SEM. Curves for the same OR responding to different odorants are shown in the same shaded box. Curves for different ORs responding to the same odorant are shown in the same outlined box. EC_{50} before and after FN application is shown in Table 2. (**B**) Percentage of OR-expressing cells that had a detectable response before (black) and immediately after (red) FN application. $^*P < 0.05$ for chi-square test performed on cell counts (table S1). (**C**) Partition coefficient [log $P_{octanol/water}$ ($P_{o/w}$)] versus fold decrease in EC_{50} upon addition of FN for each odorant tested in (A). Correlation between log $P_{o/w}$ and fold decrease in EC_{50} was significant (Pearson correlation coefficient $r = 0.70$, $P = 0.02$). Odorant structures are shown at right, with the same color coding as on the correlation plot at left.

Table 2. Hill curve fitting for dose-response curves shown in Fig. 4. "–" indicates values for dose-response curve without FN, and "+" indicates values with FN. HC, Hill coefficient.

Odorant	EC_{50}, – (μM)	EC_{50}, + (μM)	HC, –	HC, +	Max, –	Max, +
Musk ketone	21	6.9	0.95	0.85	0.14	0.14
Muscone	290	92	0.88	0.87	0.12	0.12
γ-Undecalactone (OR1D1)	150	61	1.1	1.1	0.063	0.063
γ-Undecalactone (OR2J2)	250	100	1.1	1.1	0.044	0.044
Isovaleric acid (IVA)	840	260	0.81	0.60	0.094	0.089
Methyl anthranilate (MA)	2200	710	0.80	0.70	0.11	0.11
Pentyl acetate (PA)	44	21	0.91	0.80	0.11	0.11
β-Phenylethyl alcohol	1500	1000	1.4	1.5	0.063	0.071
2,3-dimethyl pyrazine	12,000	7400	1.0	1.0	0.098	0.10
Cyclotene	1100	580	1.3	1.3	0.080	0.089
Sotolon	7.7	7.0	0.86	0.69	0.11	0.11

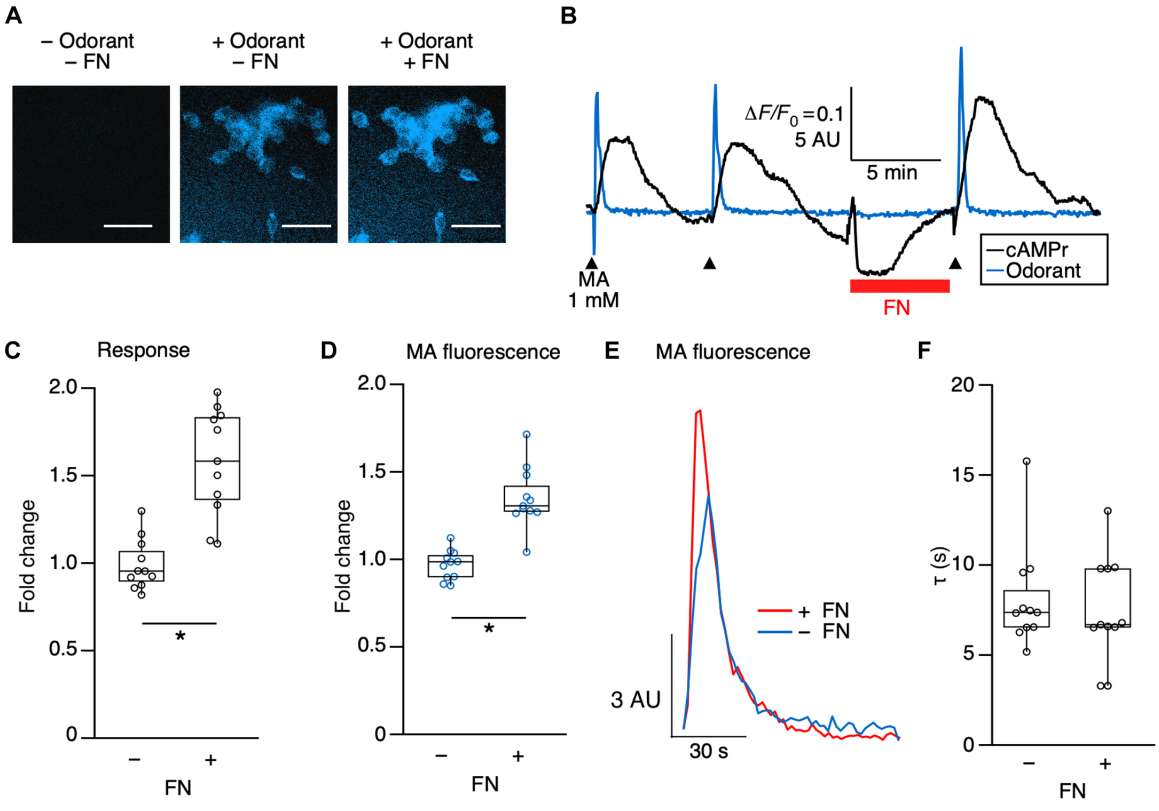

Fig. 5. FN-mediated effects on odorant molecules. (**A**) Representative fluorescence image of the odorant MA (in blue) around HEK293T/cAMPr cells before and after FN application. Scale bars, 50 μm. (**B**) Representative MA fluorescence (blue) around cell and cAMPr fluorescence (black) of an OR5P3-expressing HEK293T/cAMPr cells before and after FN application. AU, arbitrary units. (**C**) Fold change of amplitude of response to MA before and after application of FN. Ratio labeled (–) indicates the ratio of the two responses before FN application, and (+) indicates the ratio of the response after FN application to that immediately before application. (**D**) Fold change of amplitude of MA fluorescence around cell during MA stimulations before and after application of FN. Ratio labeled (–) indicates the ratio of the two peaks before sample application, and (+) indicates the ratio of the peak after FN application to that immediately before application. For (C) and (D), data are from four independent experiments ($n = 11$ cells). $^*P < 0.05$ (unpaired t-test). (**E**) Representative superimposition of the MA fluorescence around a single cell during MA stimulations immediately before (blue) and immediately after (red) FN application. (**F**) Comparison of the time constants obtained by fitting the decay phase of the MA fluorescence peak to a single exponential decay. There is no significant difference between time constant before FN application and that after FN ($P = 0.27$, unpaired t-test). Data were from four independent experiments ($n = 11$ cells).

to an exponential decay function. We compared time constants, the time for odorant fluorescence to decay to a factor of 1/*e* (to ~37%), for the pre-FN stimulation and the post-FN stimulation and found that there was no significant difference (Fig. 5F). This result indicated that FN did not affect the rate of odorant diffusion.

FN enhances the response of OSNs to vapor odorant

Having established that FN causes response enhancement in the cell-based assay, we next tested its effect on the mouse electroolfactogram (EOG), by which the odor-evoked change of local field potential at the surface of the olfactory epithelium can be measured. EOG response to odorants is tightly linked with the activity of cyclic nucleotide–gated ion channels in OSNs (*24*) and is diminished by removal of OEM (*25*). We tested whether addition of FN after OEM removal could recover the olfactory response. We found that addition of FN partially recovered the response to PA (Fig. 6, A and B) by, on average, 20% of the original response, and at most up to 40%. The lack of full recovery may be simply due to partial damage to the olfactory epithelium from the mucus-removal process but may also indicate the presence of other active factors in mouse OEM. In agreement with our results in the heterologous expression system (Fig. 2, C and D), addition of BSA did not affect the response (Fig. 6, B and C). Partial EOG response recovery by FN indicated that the response enhancement seen in the heterologous OR expression system may translate to an effect on the olfactory epithelium.

A lipocalin family protein enhances response to isovaleric acid

We next investigated the possibility of olfactory response enhancement by other OEM proteins. As a candidate, we chose lipocalin 15 (LCN15) because it is another highly abundant human OEM protein (Fig. 3D) and because the lipocalin family includes known OBPs. Although OBPs are hypothesized to increase olfactory sensitivity for the specific odorants that they can bind, odorant binding specificity has not been reported for LCN15. Thus, we tested LCN15 with four structurally diverse odorants and their respective cognate ORs, all of which we had previously tested with FN: OR51E1/isovaleric acid (IVA), OR2W1/PA, OR5P3/MA, and OR8D1/sotolon. To facilitate comparison with FN, we tested the effect of LCN15 on a concentration of odorant at which we observed significant FN-mediated response enhancement.

We found that LCN15, similar to FN, enhanced the response of OR51E1 to IVA (Fig. 7, A and B). However, LCN15 did not significantly affect the other three pairs (Fig. 7, C to H). Consistent with our initial activity-guided OEM screening using OR2W1 and PA in Fig. 3, response enhancement for OR2W1 and PA is only seen with FN (Fig. 7, C and D). However, LCN15-mediated response enhancement of OR51E1 to IVA indicates that other OEM components can also enhance odorant response for different odorant-receptor pairs. Furthermore, this result demonstrates the applicability of our cAMP imaging technique for finding and characterizing these components.

FN levels are correlated with olfactory threshold in humans

In humans, the causes of a large fraction of disorders of olfactory sensitivity are unknown; these are known as idiopathic olfactory disorders (IODs). We reasoned that since FN has odorant-response enhancing activity ex vivo and is present in high levels in human OEM, a decrease in FN levels might contribute to a subset of these disorders. First, we examined the localization of FN in the nasal mucosa by staining the human nasal olfactory mucosa–containing olfactory cleft with monoclonal anti-FN antibody (Fig. 8A, data from patient 9 in table S2). In all 10 human olfactory tissue samples (table S2), anti-FN immunoreactivity in the submucosal Bowman's glands below the olfactory epithelia was similarly observed. This result suggests that FN in the human OEM is secreted from the Bowman's glands.

Next, to examine the relationship between olfactory function and olfactory FN levels, we tested olfactory performance of volunteers (Table 2) using the T&T olfactometer, a standard clinical test in Japan. The T&T olfactometer score is the average of the sensitivity threshold score for five odorants (cyclotene, β-phenylethylalcohol, IVA, γ-undecalactone, and scatole) with higher scores indicative of poorer sensitivity. Volunteers were considered to have an IOD if they met the following criteria: (i) reduced olfactory sensitivity as indicated by a score of >2 on the T&T olfactometer and (ii) no cause for the disorder found upon medical examination. We found a significant difference between OEM FN levels in patients with IOD (seven males and nine females) and age-matched controls (eight males and eight females; Fig. 8B and fig. S6). The results of our human study,

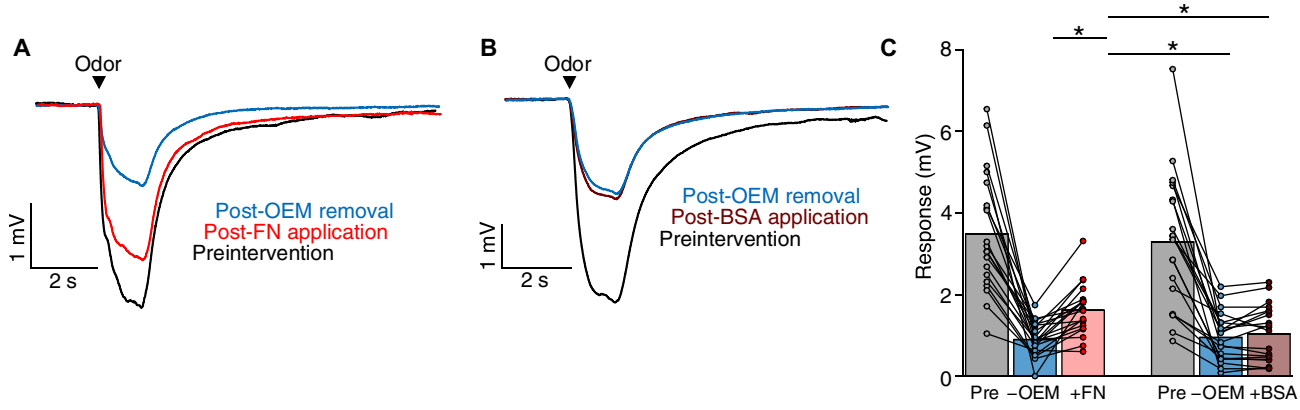

Fig. 6. Partial recovery of EOG response to PA by FN. (**A**) Representative traces for EOG response to a 1-s stimulation with headspace of 100 μM PA from a single animal before OEM removal (preintervention; black), after OEM removal (blue), and after FN (300 μg/ml) addition (red). (**B**) Representative traces for response to a 1-s stimulation with headspace of 100 μM PA from a single animal before OEM removal (black), after OEM removal (blue), and after BSA (300 μg/ml) addition (red). (**C**) Quantification of responses for 20 animals under FN condition and 20 animals under BSA condition. *$P < 0.05$, post hoc Tukey test with mixed-model ANOVA.

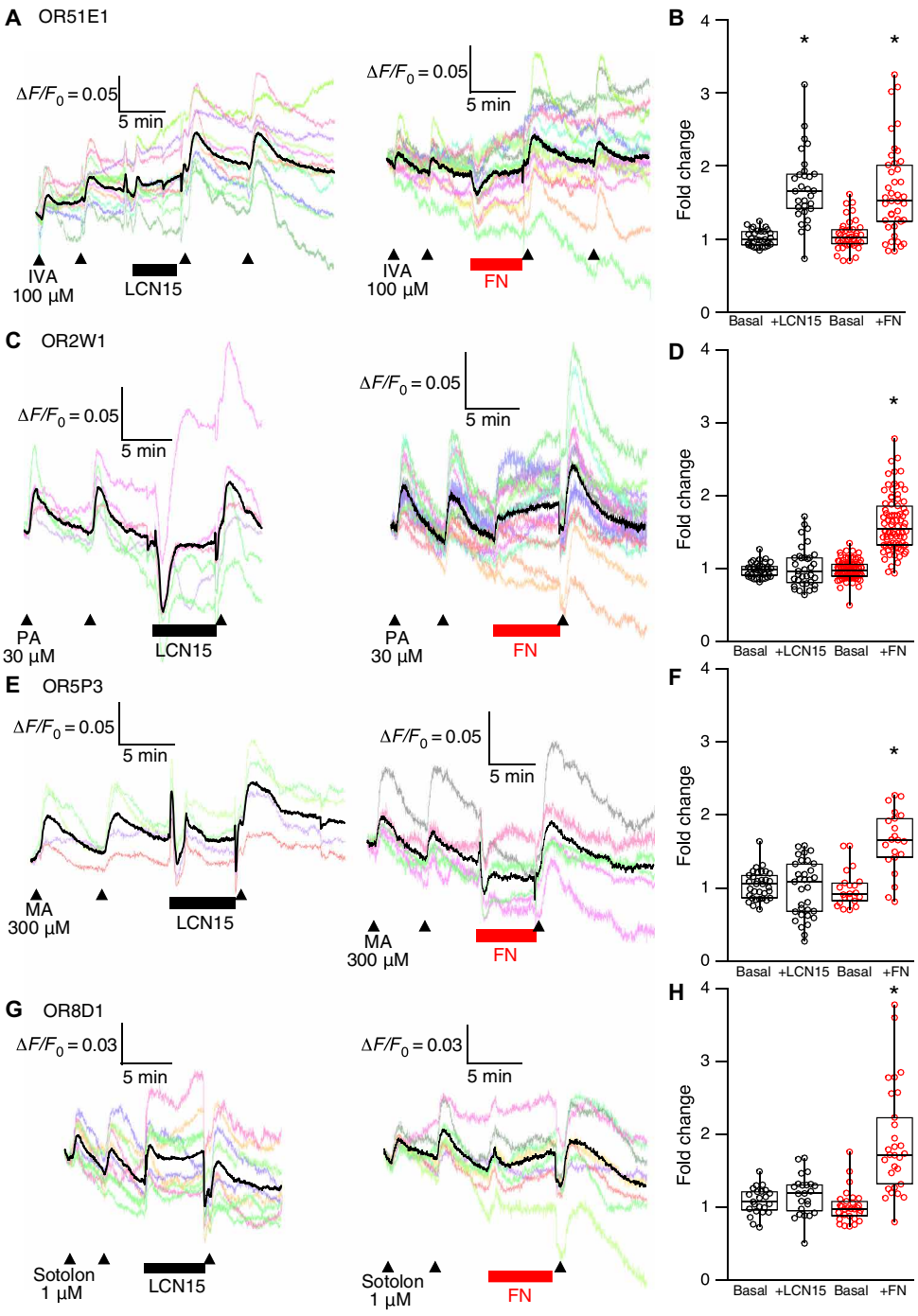

Fig. 7. Comparison of the effects of FN and LCN15 on odorant response for four odorant-OR pairs. (**A**) Representative cAMP responses to 100 μM IVA in OR51E1-expressing HEK293T/cAMPr cells before and after application of LCN15 ($n = 12$) or FN ($n = 16$). (**B**) Fold change of amplitude of IVA-evoked response before and after application of FN or LCN15. Basal ratio indicates the ratio of the two responses before application of protein. +FN or +LCN15 indicates the ratio of the first response after application to the response immediately before application of the specified protein. Data were obtained from three independent experiments per protein (FN, $n = 41$ cells; LCN15, $n = 30$ cells). In (B), (D), (F), and (H), $^*P < 0.05$, post hoc Tukey test with one-way ANOVA. (**C**) Representative cAMP responses to 30 μM PA in OR2W1-expressing HEK293T/cAMPr cells before and after application of LCN15 ($n = 6$) or FN($n = 17$). (**D**) Fold change of amplitude of PA-evoked response before and after application of FN or LCN15. For FN, data were obtained from five independent experiments ($n = 81$ cells); for LCN15, data were obtained from four independent experiments ($n = 35$ cells). (**E**) Representative cAMP responses to 300 μM MA in OR5P3-expressing HEK293T/cAMPr cells before and after application of LCN15 ($n = 4$) or FN ($n = 6$). (**F**) Fold change of amplitude of MA-evoked response before and after application of FN or LCN15. For FN, data were obtained from three independent experiments ($n = 29$ cells); for LCN15, data were obtained from seven independent experiments ($n = 33$ cells). (**G**) Representative cAMP responses to 1 μM sotolon in OR8D1-expressing HEK293T/cAMPr cells before and after application of LCN15 ($n = 10$) or FN ($n = 13$). (**H**) Fold change of amplitude of sotolon-evoked response before and after application of FN or LCN15. Data were obtained from three independent experiments per protein (FN, $n = 29$ cells; LCN15, $n = 23$ cells).

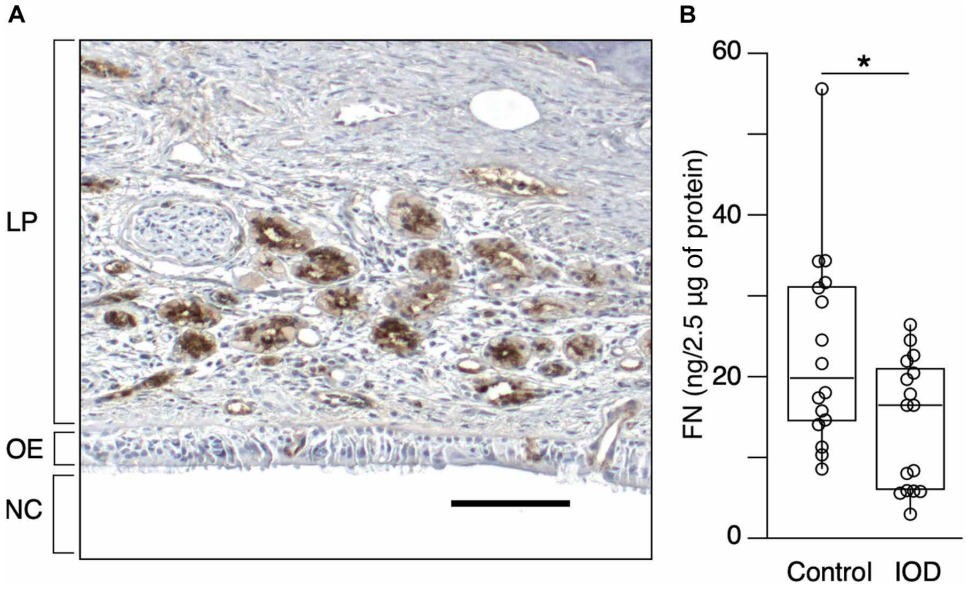

Fig. 8. Olfactory FN in human individuals. (**A**) A representative photomicrograph of olfactory cleft mucosa immunostained with anti-FN antibody. Immunoreactivity was visualized using horseradish peroxidase (HRP)–conjugated anti-mouse immunoglobulin G (IgG) secondary antibody and diaminobenzidine (DAB) reaction (brown color). LP, lamina propria; OE, olfactory epithelium; NC, nasal cavity. Scale bar, 100 µm. (**B**) Comparison of FN levels in the olfactory mucus samples of patients with IOD (nine females and seven males) and age-matched normosmic controls (eight females and eight males). *$P < 0.05$, unpaired *t*-test.

while limited by a small sample size, are consistent with an olfactory sensitivity–enhancing role for FN in vivo and with a contribution from OEM FN deficiency in a subset of IODs.

DISCUSSION

OEM has long been thought to play a role in olfactory sensitivity, but the identity of the sensitivity-enhancing factor(s) has remained elusive. In this work, we identified FN as an olfactory sensitivity–regulating factor in OEM, using a real-time cAMP measurement technique. We showed that FN decreases EC_{50} of the cognate OR for a wide range of chemically diverse odorants. We found that in the presence of FN, the amount of odorant around cells transiently increased, suggesting that this increase may be the mechanism underlying improved sensitivity of odorant response. We demonstrate that FN also shows response-enhancing activity in olfactory epithelium, where it can partially substitute for the enhancer function of OEM. Last, decreased FN levels in human OEM may contribute to IODs.

Reconstructing olfactory sensitivity has proven a sizeable challenge to both basic science research and to the development of biohybrid odorant sensors (*2*, *4*). Here, we show that FN from OEM can directly increase sensitivity of OR response to cognate odorants. Partial rescue of EOG responses by FN after OEM removal suggested that FN can, to some extent, serve as a substitute for OEM, raising the possibility that artificial OEM can be used to reconstruct in vivo sensitivity. In addition, olfactory response enhancement by LCN15 indicates that multiple active factors exist in OEM. The fact that some odorants were affected by FN but not LCN15 suggests that different active factors may have distinct but partially overlapping odorant "specialties," analogous to how different ORs recognize distinct but partially overlapping sets of odorants. Comprehensive identification of key elements in OEM is required to fully elucidate and reconstruct the superior sensing mechanism of olfaction.

Our results suggest that the sensitivity of olfactory responses can be regulated by interactions between extracellular components in OEM, such as FN, and odorants. These extracellular components might affect the apparent association constant of odorant to OR and/or diffusion constant of the odorants, thus reducing the EC_{50}. We found that FN did not affect the diffusion of the autofluorescent odorant MA but that it increased the amount of odorant on the surface of cells, which could enhance the binding of MA and OR5P3 and thus result in improved sensitivity. To achieve this transient increase in odorant, FN may bind odorants with weak affinity and a fast dissociation rate, as it has been shown to do for the small molecule 2,2-diphenylethylamine (*21*). In addition, FN may act as a molecular crowding agent. Protein/ligand interaction sensitivity has been shown to rise more than 1000 times upon reduction of reaction volume to femtoliter level (*26*). Because FN is a large (>200 kDa) protein, it may reduce the volume available for odorant-OR interactions and thus increase sensitivity by a similar mechanism.

The effect of FN on sensitivity also sheds light on the well-known but seemingly paradoxical phenomenon that odorants are generally hydrophobic, despite the fact that they must dissolve into the aqueous OEM layer to be recognized at the OSNs. In contrast, very hydrophilic molecules ($\log P_{o/w} < -1$) are generally not odorous, even when they fall into the same volatility and molecular weight ranges as odorants (*22*, *27*). Previous studies have shown that the more hydrophobic the odorant, the better it sorbs from air into OEM compared to into water, but whether this phenomenon could affect OR response and whether specific OEM factors were responsible remained unknown (*28*–*30*). Here, we show that sensitivity enhancement by OEM FN is stronger for more hydrophobic odorants. In vivo, FN (and potentially other factors) may efficiently boost sensitivity to hydrophobic molecules, while having no effect or negative effect on very hydrophilic ones. Our result thus suggests that OEM-odorant interactions may explain why hydrophobic molecules can be odorous.

A crucial factor in our discovery of the effect of FN on sensitivity was our cAMP imaging technique. Our assay permits both spatiotemporal analysis of cAMP response and sequential and repeated chemical application on a timescale closer to in vivo than established OR heterologous expression assays. Although in vivo olfaction is characterized by an odorant-receptor interaction time under 1 s (*22*), the OR heterologous expression assay in widest use today is a luciferase expression–based plate assay in which odorant stimulation is conducted for 3 to 4 hours (*31*). When this luciferase assay was used, the effect of LCN15 on the OR51E1-IVA pair could not be detected (*9*). Attempts to test the effect of human OEM samples on OR response using the luciferase assay have also proven unsuccessful (*32*). In contrast, our cAMP imaging technique allowed us to detect response enhancement by both LCN15 (for OR51E1 with IVA) and by OEM samples (for multiple OR-odorant pairs), which latter led to the discovery of sensitivity enhancement by FN. Thus, we anticipate that our technique will continue to prove useful for discovery and characterization of additional OEM factors.

Last, understanding the role of FN and other sensitivity-enhancing factors from OEM may also shed light on disorders of olfactory sensitivity, many of which remain idiopathic. In the OEM of normosmic human individuals, FN is reported to be among the top 10 most abundant proteins (*9*), and across human tissues, OEM has the third-highest FN expression levels (*7*). We found that patients with IOD had significantly lower FN levels compared to age-matched normosmic controls. Disorders falling under the umbrella of IOD likely span a variety of distinct conditions with different causes, and our human survey likely also includes patients whose IOD is unrelated to FN levels. Nonetheless, our results suggest that FN may be involved in human olfaction. Together, this work sheds light on the role of OEM and FN in olfactory sensitivity and lays a foundation for using FN for sensitivity enhancement in biohybrid odorant sensors and in olfactory therapeutics.

MATERIALS AND METHODS

Establishment of the HEK293T/cAMPr cell line

HEK293T cells were cultured in Dulbecco's modified Eagle's medium (04129775, Wako) supplemented with 10% fetal bovine serum (BioWest) and were grown in a 37°C incubator containing 5% CO_2. cDNA encoding a fluorescent sensor for cAMP, cAMPr (*18*), was purchased from Addgene and subcloned into a piggyback transposon vector (PB514B-2, SBI). The cAMPr vector was cotransfected with Super piggyback transposase transient expression vector (PB210-PA-1, SBI) into HEK293T cells by using X-tremeGENE HP (63662-44001, Merck). Starting 3 days after transfection, puromycin selection (2.5 μg/ml) was applied for 2 months. Seven colonies were picked and were checked using functional expression of Olfr73.

cAMP imaging in HEK293T/cAMPr cells

HEK293T cells constitutively expressing the cAMP sensor cAMPr were seeded in 35-mm glass-based dishes (Iwaki) with collagen coating (Cellmatrix Type I-C, Nitta Gelatin) and transfected with 2 μg of pME18S-Rho-tag OR and 0.5 μg of pME18S-RTP1S using X-tremeGENE HP (6366244001, Merck). "Rho-tag" indicates the N-terminal 20 amino acids of bovine rhodopsin. Forty-six to 52 hours after transfection, medium was replaced with Ringer's solution (140 mM NaCl, 5.6 mM KCl, 5 mM Hepes, 2 mM sodium pyruvate, 1.25 mM KH_2PO_4, 2 mM $CaCl_2$, 2 mM $MgCl_2$, and 9.4 mM D-glucose, pH adjusted to 7.4 with NaOH), and cells were allowed to come to room temperature (10 to 20 min) before imaging.

Odorant solutions were applied to the cells using a custom-made perfusion system. Odorant stimulation was performed in 10-s duration unless otherwise indicated. For PA [A0021, Tokyo Chemical Industry (TCI)], eugenol (A0232, TCI), cyclotene (H0469, TCI), IVA (M0182, TCI), MA (A0500, TCI), sotolon (W363495-25G-K, Sigma-Aldrich), β-phenylethyl alcohol (P0084, TCI), and 2,3-dimethylpyrazine (D1525, TCI), odorants were diluted directly into Ringer's solution, while musk ketone (60720, Fluka), γ-undecalactone (U0003, TCI), and muscone (M2611, TCI) were prepared as a 100 mM stock in dimethyl sulfoxide, which was then diluted into Ringer's solution.

OEM samples, FN (FIBRP-RO 11080938001, Roche), LCN15 [prepared as described in (*9*)], BSA (014-15151, Wako), and buffer control were applied to cells using a syringe pump (KDS-100, 78-0100 J, KD Scientific) equipped with a 1-ml syringe (Terumo). To add test substance, perfusion was paused, and 200 μl of test substance was delivered over 1 min. Subsequently, either (i) perfusion was immediately restarted or (ii) the test substance was incubated with cells for 5 min before restarting perfusion. For dose-response curves in Fig. 4, the effect of FN on the dose-response curve was measured by performing separate experiments for each odorant concentration.

Fluorescence was measured with an Olympus IX3 microscope equipped with autofocus, a Hamamatsu ORCA R2 camera (C10600, Hamamatsu Photonics) and a light-emitting diode light source (pE-340fura, CoolLED Ltd.). Data acquisition was carried out using HCImage (Hamamatsu Photonics), with a sampling rate of 0.5 to 1 frames/s, except Fig. 1C. Analysis was carried out using Igor Pro 9.0 (WaveMetrics).

Two-color imaging of MA and cAMP response

For simultaneous imaging of MA autofluorescence and cAMP response, cells were seeded in 35-mm glass-based dishes (Iwaki) with poly-L-ornithine coating (163-27421, Wako). Transfection, stimulation, and fluorescence measurement were carried out as described in the "cAMP imaging in HEK293T/cAMPr cells" section, except that MA fluorescence at 380-nm excitation and 430-nm emission was also measured. Delay between measurement of cAMPr fluorescence and MA fluorescence was 1 s. For MA fluorescence, to account for background from MA above the cell layer, fluorescence around cells was quantified as fluorescence of a cell-containing region of interest minus fluorescence in a cell-free area of the field of view.

Collection of human olfactory mucus and tissue samples

Procedures involving human individuals were approved by the study review committee at Ajinomoto Co. Inc. (nos. 2018-009 and 2018-026) and the Institutional Review Boards at the University of Tokyo Hospital (nos. 2018092NI, 2019073NI, 2024224NI, and 2024228NI) and Mie University School of Medicine (no. H2019-16), respectively. All procedures involving human individuals were conducted according to the Declaration of Helsinki.

Human individuals

To collect nasal mucus samples, both healthy individuals and individuals with olfactory impairment were enrolled between November 2018 and December 2019. Individuals, who included patients, their families, and hospital employees, were recruited by advertisement in the University of Tokyo Hospital and compensated for their time and effort. All individuals provided written informed consent before participation in this study. Individuals completed medical history questionnaires to collect demographic data such as age, gender,

medical comorbidities, and past/current smoking exposure. Characteristics of the individuals are summarized in Table 2.

Diagnosis of olfactory disorders was based on medical history, endoscopic inspection of the nasal cavity, computed tomography scanning, and olfactory test. These modalities can exclude specific causes of olfactory disorders such as allergy, chronic rhinosinusitis, postviral olfactory disorder, and head trauma. If the patients had olfactory decline but its cause could not be diagnosed by those modalities, then olfactory dysfunction was diagnosed as idiopathic.

Irrigation of the superior nasal cavity by saline

To obtain mucus from the olfactory cleft, we irrigated the olfactory cleft with saline as described in (*16*). Briefly, the participants were asked to sit in a prone position with knees bent and the top of the forehead on the floor. One milliliter of saline at 37°C was introduced into the nostril on one side and left for 1 min. The participant then returned to an upright position, and the liquid that exited the nostril was collected and immediately frozen in liquid nitrogen and stored at −80°C.

Human nasal tissue

To examine the localization of FN in the human nasal mucosa, archival nasal tissues containing olfactory cleft and cribriform plate ($n = 10$) were used. All tissues were surgical specimens from patients who underwent resection of the skull base (including the cribriform plate) for the treatment of tumors. The demographic data of these patients are shown in table S1. In accordance with Institutional Review Board instruction, we contacted the patients and obtained written informed consent for the study. In cases when we were unable to contact the patient at the time of study entry, we offered the option for patients (or, in the case of death, their descendants) to opt out.

All specimens had previously been decalcified and embedded in paraffin. Four-micrometer-thick sections were cut from the specimens and mounted on MAS Coat slides (Matsunami Glass, Osaka, Japan).

Olfactory acuity testing

Olfactory acuity was scored using the average of the recognition thresholds of the T&T olfactometer (*33*) with a slight modification. The T&T olfactometer is the standard olfactory assessment test in Japan and uses the following five odorants: (i) β-phenyl ethyl alcohol, (ii) cyclotene (methyl cyclopentenolone), (iii) IVA, (iv) γ-undecalactone, and (v) skatole (Daiichi Yakuhin Sangyo, Tokyo, Japan). The concentrations of each odorant ranged over eight degrees of intensity (−2 to 5) except for cyclotene, which ranged over seven degrees of intensity (−2 to 4). During the test, patients sniffed strips of paper dipped in different concentrations of each of the five odorants.

The recognition threshold was defined as the lowest concentration at which the odor could be identified. We started the presentation of each odor at concentration level 2. When the individuals could identify all of the five odorants at level 2, the individuals were categorized as having normal olfaction, in accord with the definition used in previous studies (*34*). If individuals could not identify any of the odorants, odorants were presented in increasing concentration until identification became possible. If individuals could not identify the highest concentrations (five for i, iii, iv, and v and four for ii), then their threshold for that odorant was scored as six for i, ii, iv, and v and five for ii. The recognition thresholds of the five odorants were averaged to give the T&T score.

Enzyme-linked immunosorbent assay

The concentration of FN in nasal mucus samples was measured using TaKaRa FN enzyme-linked immunosorbent assay kit (MK115, Takara Bio Inc., Shiga, Japan) according to the manufacturer's instructions.

Immunohistochemistry

For immunostaining, human nasal tissue sections were deparaffinized and then rehydrated through a xylene and ethanol series. Sections were then immersed in antigen retrieval solution (S1700, Dako Cytomation) and then autoclaved at 121°C for 20 min for retrieval of antigens.

After antigen retrieval, endogenous peroxidase activity was blocked by treatment with 3% hydrogen peroxide in methanol for 10 min at room temperature. The sections were then incubated for 10 min with a blocking solution (Blocking-One Histo, Nakarai Tesque, Tokyo) at room temperature, followed by incubation with mouse monoclonal anti-FN antibody (68042-1-Ig, Proteintech, Tokyo, Japan; 1:3000 in tris-buffered saline with 0.1% of Tween 20 and 5% blocking solution) at room temperature for 1 hour. After washing with phosphate-buffered saline (PBS) (pH 7.4), the sections were incubated for 30 min at room temperature with horseradish peroxidase (HRP)–conjugated anti-mouse immunoglobulin G (IgG) secondary antibody (Simple Stain MAX PO [M], ready-to-use, Nichirei, Tokyo, Japan) and then washed again with PBS. Immunoreactivity was visualized using diaminobenzidine (DAB) (Simple Stain DAB, ready-to-use, Nichirei). After washing with distilled water, the sections were counterstained with hematoxylin and then dehydrated and mounted. As a negative control, the primary antibody was omitted from the reaction; no obvious labeling corresponding to immunostaining by the primary antibody was observed.

Stained sections were examined under bright-field illumination using an E800 microscope (Nikon, Tokyo, Japan) and photographed using a digital camera (AxioCam, Carl Zeiss, Tokyo, Japan). Images were processed in Adobe Photoshop, adjusting only brightness, contrast, and color balance.

Ultrafiltration of olfactory mucus sample and purification of FN

Ultrafiltration was carried out using a 100-kDa molecular weight cutoff (MWCO) Centrisart I centrifugal ultrafiltration unit (13269E, Sartorius). After ultrafiltration, the >100-kDa fraction was adjusted to the original sample volume by addition of Ringer. Fractions were lyophilized immediately after preparation and stored at −80°C until use.

For purification of FN, ultrafiltration was performed as described above. Immediately after ultrafiltration, the >100-kDa fraction was applied to a 5 mm–by–50 mm polypropylene Muromac column (Muromachi Chemicals Incorporated) loaded with 230 μl of Gelatin Sepharose 4B (17095601, Cytiva). Running buffer was glucose-free Ringer's solution. Wash buffer was 1 M NaCl in running buffer. Elution buffer was 1 M arginine in running buffer. After elution, a 100-kDa MWCO Centrisart I unit was used to concentrate eluate and remove arginine.

Western blotting

Samples were subjected to SDS-PAGE on a 7.5% acrylamide gel at constant current of 30 mA. Bovine plasma FN (42805, ThermoFisher) was used as positive control. To denature proteins, samples were incubated at 95°C for 5 min with 1× sample buffer [0.25 M tris-HCl, 75 mM SDS, 7% glycerol, 5% β-mercaptoethanol, and 2.5% bromophenol blue (pH 6.8)] before loading on the acrylamide gel. Proteins were transferred to polyvinylidene difluoride membrane (0.2 μm; EH-2222, Pall Corporation FluoroTrans W Membrane) using a Trans-Blot SD Semi-Dry Transfer Cell (1703940, Bio-Rad) at

15 V for 2 hours using Bjerrum and Schafer-Nielsen transfer buffer with SDS [48 mM tris, 39 mM glycine, 20% (v/v) methanol, and 0.0375% SDS].

After transfer, the membrane was blocked with 4% BSA (A2153-50G, Sigma-Aldrich) dissolved in TBS-T [25 mM tris-HCl, 137 mM NaCl, 2.7 mM KCl, and 0.1% Tween 20 (P9416-50ML, Sigma-Aldrich) (pH 7.4)] for 1 hour shaking at room temperature. Primary antibody (mouse anti-FN, 51-9001967, BD Transduction Laboratories) incubation was performed at 1:2000 for 1 hour at room temperature. After washing with TBS-T, the membrane was incubated with HRP-conjugated secondary antibody (goat anti-mouse IgM & IgG, 4050-05, Southern Biotech) at 1:5000 dilution for 1 hour at room temperature. To visualize signal, the membrane was incubated with ImmunoStar LD (296-69901, Wako), followed by detection of chemiluminescence signals with an ImageQuant LAS 4000 mini system (GE Healthcare).

Animals

Male Slc:ICR mice were purchased from SLC Japan and were 6 to 7 weeks of age. Mice were kept in an approved animal room on a 12-hour light/12-hour dark cycle, with standard chow provided ad libitum. All animal procedures were performed in accordance with the animal care guidelines approved by the University of Tokyo (study approval number P25-056).

Electrophysiology

Mice were injected with a lethal dose of pentobarbital. Immediately after death, mice were decapitated and the skulls bisected along the midsagittal plane. To expose the turbinates, the overlaying septal bone and epithelium were removed. If both left and right sides of head were intact, then both were used, with one side chosen at random for testing FN and the other for BSA.

After dissection, the head was placed in a 1% agar bed containing Ringer's solution. Odorant (PA, Wako) was delivered via a 1.0-s puff of N_2 gas from the headspace of a 60-ml glass vial containing 100 μM PA dissolved in water. Recordings were taken from endoturbinates II and III because the PA response amplitude was found to be greatest at these sites. Electrical potential changes were recorded from the epithelium using a glass pipette filled with Ringer's solution and 1% agar, which was connected by an Ag/AgCl bridge to an ac/dc differential amplifier (DP-301, Warner Instrument Corporation). As a reference electrode, a second Ag/AgCl bridge was connected to another glass pipette, which was inserted into the agar bed. Electrical signals were collected using a PowerLab/8SP (ADInstruments).

OEM removal was carried out using a medical sponge (Tafpott 3 TTP3-M10, HOGY) cut into an approximately 2 mm–by–0.5 mm–by–0.5 mm wedge with a tapered tip. After lifting the recording electrode, the sponge was applied lightly to the recording site for 3 to 5 s. Sponge application was repeated five to eight times per site before the electrode was replaced.

Mouse plasma FN (AB92784, Abcam) or BSA (014-15151, Wako) was delivered at 300 μg/ml by drawing up ~0.5 μl of solution in a 28-gauge Microfil needle (MF26G67-5, World Precision Instruments), pushing out a fraction of the volume to form a drop of liquid at the tip of the needle, and gently applying the droplet directly to the turbinate proximal to the recording electrode. Excess liquid was drawn away by gently touching an ~0.2- to 0.5-mm-width strip of KimWipe to the meniscus of the added liquid at a site distal to the electrode.

After test substance application, responses to the headspace of 100 μM PA were measured periodically for 10 to 20 min, and the response with greatest amplitude in that time period was chosen as the postapplication response. For each individual, the wait time after FN application was matched to the wait time after BSA application.

Physicochemical descriptors

Physicochemical descriptors of odorants were gathered from the online databases PubChem and Good Scents Company and in cases where no values could be found in those databases, from product datasheets provided by makers of odorant compounds. We chose to use experimental over calculated values whenever possible.

Statistical analyses

Statistical analyses were performed using Igor Pro (version 9.05, WaveMetrics) except for χ^2 testing and correlation analysis, which were performed using Prism (version 10.3.1, GraphPad Software). Details, including sample size and *P* values, are described in each figure legend.

Supplementary Materials

The PDF file includes:

Figs. S1 to S6
Legend for table S1
Table S2

Other Supplementary Material for this manuscript includes the following:

Table S1

REFERENCES AND NOTES

1. L. Buck, R. Axel, A novel multigene family may encode odorant receptors: A molecular basis for odor recognition. *Cell* **65**, 175–187 (1991).
2. J. W. Cave, J. K. Wickiser, A. N. Mitropolous, Progress in the development of olfactory-based bioelectronic chemosensors. *Biosens. Bioelectron.* **123**, 211–222 (2019).
3. J.-M. Heydel, P. Faure, F. Neiers, Nasal odorant metabolism: Enzymes, activity and function in olfaction. *Drug Metab. Rev.* **51**, 224–245 (2019).
4. Y. Hirata, H. Oda, T. Osaki, S. Takeuchi, Biohybrid sensor for odor detection. *Lab Chip* **21**, 2643–2657 (2021).
5. J. Plendl, F. Sinowatz, Glycobiology of the olfactory system. *Acta Anat.* **161**, 234–253 (1998).
6. H. Débat, C. Eloit, F. Blon, B. Sarazin, C. Henry, J.-C. Huet, D. Trotier, J.-C. Pernollet, Identification of human olfactory cleft mucus proteins using proteomic analysis. *J. Proteome Res.* **6**, 1985–1996 (2007).
7. T. Olender, I. Keydar, J. M. Pinto, P. Tatarskyy, A. Alkelai, M.-S. Chien, S. Fishilevich, D. Restrepo, H. Matsunami, Y. Gilad, D. Lancet, The human olfactory transcriptome. *BMC Genomics* **17**, 619 (2016).
8. K. Yoshikawa, H. Wang, C. Jaen, M. Haneoka, N. Saito, J. Nakamura, N. D. Adappa, N. A. Cohen, P. Dalton, The human olfactory cleft mucus proteome and its age-related changes. *Sci. Rep.* **8**, 17170 (2018).
9. C. Ijichi, K. Kondo, M. Kobayashi, A. Shirasawa, K. Shimbo, K. Nakata, Y. Maruyama, Y. Ihara, Y. Kawato, T. Mannen, R. Takeshita, Y. Kikuchi, Y. Saito, T. Yamasoba, Lipocalin 15 in the olfactory mucus is a biomarker for Bowman's gland activity. *Sci. Rep.* **12**, 9984 (2022).
10. R. Henkin, N. Talal, A. Larson, C. Mattern, Abnormalities of taste and smell in Sjogren's syndrome. *Ann. Intern. Med.* **76**, 375–383 (1972).
11. U. F. Kamel, P. Maddison, R. Whittaker, Impact of primary Sjorgen's syndrome on smell and taste: Effect on quality of life. *Rheumatology* **48**, 1512–1514 (2009).
12. Y. E. Topan, B. Bozkurt, S. Yılmaz, Ç. Elsürer, S. Gorcuyeva, M. K. Bozkurt, Olfactory dysfunction in primary Sjorgen's syndrome and its correlation with dry eye. *Acta Otorhinolaryngol. Ital.* **41**, 443–449 (2021).
13. N. Fukuda, M. Shirasu, K. Sato, E. Ebisui, K. Touhara, K. Mikoshiba, Decreased olfactory mucus secretion and nasal abnormality in mice lacking type 2 and type 3 IP3 receptors. *Eur. J. Neurosci.* **27**, 2665–2675 (2008).
14. J.-M. Heydel, A. Coelho, N. Thiebaud, A. Legendre, A.-M. Le Bon, P. Faure, F. Neiers, Y. Artur, J. Golebiowski, L. Briand, Odorant-binding proteins and xenobiotic metabolizing enzymes: Implications in olfactory perireceptor events. *Anat. Rec.* **296**, 1333–1345 (2013).
15. P. Pelosi, The role of perireceptor events in vertebrate olfaction. *Cell. Mol. Life Sci.* **58**, 503–509 (2001).

16. C. Ijichi, H. Wakabayashi, S. Sugiyama, Y. Ihara, Y. Nogi, A. Nagashima, S. Ihara, Y. Niimura, Y. Shimizu, K. Kondo, K. Touhara, Metabolism of odorant molecules in human nasal/oral cavity affects the odorant perception. *Chem. Senses* **44**, 465–481 (2019).
17. T. Nakamura, Y. Noumi, H. Yamakawa, A. Nakamura, D. Wen, X. Li, X. Geng, K. Sawada, T. Iwasa, Enhancement of the olfactory response by lipocalin Cp-Lip1 in newt olfactory receptor cells: An electrophysiological study. *Chem. Senses* **44**, 523–533 (2019).
18. C. R. Hackley, E. O. Mazzoni, J. Blau, cAMPr: A single-wavelength fluorescent sensor for cyclic AMP. *Sci. Signal.* **11**, eaah3738 (2018).
19. K. Kajiya, K. Inaki, M. Takana, T. Haga, H. Kataoka, K. Touhara, Molecular bases of odor discrimination: Reconstruction of olfactory receptors that recognize overlapping sets of odorants. *J. Neurosci.* **21**, 6018–6025 (2001).
20. J. D. Mainland, A. Keller, Y. R. Li, T. Zhou, C. Trimmer, L. L. Snyder, A. H. Moberly, K. A. Adipietro, W. L. L. Liu, H. Zhuang, S. Zhan, S. S. Lee, A. Lin, H. Matsunami, The missense of smell: Functional variability in the human odorant receptor repertoire. *Nat. Neurosci.* **17**, 114–120 (2014).
21. J. Scheuermann, A. Volonterio, O. Zerbe, M. Zanda, D. Neri, Discovery and investigation of lead compounds as binders to the extra-domain B of the angiogenesis marker, fibronectin. *Drug Dev. Res.* **58**, 268–282 (2003).
22. H. Boelens, Structure-activity relationships in chemoreception by human olfaction. *Trends Pharmacol. Sci.* **4**, 421–426 (1983).
23. C. Liu, K. Hayashi, Visualization of controlled fragrance release from cyclodextrin inclusion complexes by fluorescence imaging. *Flavour Fragr. J.* **29**, 356–363 (2014).
24. L. J. Brunet, G. H. Gold, J. Ngai, General anosmia caused by a targeted disruption of the mouse olfactory cyclic nucleotide-gated cation channel. *Neuron* **17**, 681–693 (1996).
25. T. Shibuya, Dissociation of olfactory neural response and mucosal potential. *Science* **143**, 1338–1340 (1964).
26. K. V. Tabata, Y. Minagawa, Y. Kawaguchi, M. Ono, Y. Moriizumi, S. Yamayoshi, Y. Fujioka, Y. Ohba, Y. Kawaoka, H. Noji, Antibody-free digital influenza virus counting based on neuraminidase activity. *Sci. Rep.* **9**, 1067 (2019).
27. E. J. Mayhew, C. J. Arayata, R. C. Gerkin, J. D. Mainland, Transport features predict if a molecule is odorous. *Proc. Natl. Acad. Sci. U.S.A.* **119**, e2116576119 (2022).
28. D. E. Hornung, M. M. Mozell, J. A. Serio, "Olfactory mucus/air partitioning of odorant," in *Olfaction and Taste* (Information Retrieval Ltd., 1980), pp. 167–170.
29. D. E. Hornung, S. L. Youngentob, M. M. Mozell, Olfactory mucosa/air partitioning of odorants. *Brain Res.* **413**, 147–154 (1987).
30. D. B. Kurtz, K. Zhao, D. E. Hornung, P. W. Scherer, Experimental and numerical determination of odorant solubility in nasal and olfactory mucosa. *Chem. Senses* **29**, 763–773 (2004).
31. H. Zhuang, H. Matsunami, Evaluating cell-surface expression and measuring activation of mammalian odorant receptors in heterologous cells. *Nat. Protoc.* **3**, 1402–1413 (2008).
32. T. Shirai, D. Takase, J. Yokoyama, K. Nakanishi, C. Uehara, N. Saito, A. Kato-Namba, K. Yoshikawa, Functions of human olfactory mucus and age-dependent changes. *Sci. Rep.* **13**, 971 (2023).
33. T. Miwa, K. Ikeda, T. Ishibashi, M. Kobayashi, K. Kondo, T. Ogawa, H. Shiga, M. Suzuki, T. Tsuzuki, A. Furuta, Y. Motoo, S. Fujieda, Y. Kurono, Clinical practice guidelines for the management of olfactory dysfunction. *Auris Nasus Larynx* **46**, 653–662 (2019).
34. H. Shiga, K. Okuda, J. Taki, N. Watanabe, H. Tonami, S. Kinuya, T. Miwa, Nasal thallium-201 uptake in patients with parosmia with and without hyposmia after upper respiratory tract infection. *Int. Forum Allergy Rhinol.* **9**, 1252–1256 (2019).

Acknowledgments: We thank M. Kobayashi (Mie University) and Y. Saito (The University of Tokyo) for recruiting the participants and collecting/preparing specimens of human olfactory cleft mucosa and S. Kikuta (Nihon University), Y. Shimizu (Teikyo University), H. Nishijima, and M. Kishimoto-Urata (The University of Tokyo) for collecting nasal mucus. We thank members of the Touhara laboratory for discussion and advice. **Funding:** This work was supported by MEXT Quantum Leap Flagship Program (MEXT Q-LEAP) grant number JPMXS0120330644 (to K.T.), JSPS KAKENHI grant number 23H05410 (to K.T.), JSPS KAKENHI grant numbers 19H02531 and 23H00244 (to K.S.), Takeda Science Foundation (to K.S.), Mishima Kaiun Memorial Foundation (to K.S.), and JST SPRING grant number JPMJSP2108 (to S.C.) **Author contributions:** Conceptualization: K.S., S.C., K.K., and K.T. Investigation: S.C., K.K., and K.S. Methodology: K.S., S.I., K.K., and K.T. Software: K.S. Formal analysis: K.S. Resources: K.S. and C.I. (LCN15 recombinant protein and related information; C.I. was not involved in any animal experiments). Funding acquisition: K.S. and K.T. Supervision: K.T. Visualization: S.C. and K.T. Project administration: K.T. Writing—original draft: S.C., K.S., and K.K. Writing—review and editing: S.C., K.S., K.K., S.I., C.I., and K.T. **Competing interests:** S.C. and K.T. have filed a patent application for the use of FN as an odorant-sensitivity enhancing additive. C.I. is an employee of Ajinomoto Co. Inc. and received research support from Ajinomoto Co. Inc. All other authors declare that they have no competing interests. **Data and materials availability:** All data needed to evaluate the conclusions in the paper are present in the paper and/or the Supplementary Materials. Requests for reagents should be directed to and fulfilled by the corresponding authors.

Submitted 19 November 2024
Accepted 9 April 2025
Published 14 May 2025
10.1126/sciadv.adu7271